Evaluation of cytotoxicity

The cytotoxicity of cationized-gelatin–plasmid DNA complexes was evaluated. Briefly, L929 cells were cultured with the complexes prepared at different N^+/P^- mixing ratios for 24 h. After that, the culture medium was discarded and 1 ml fresh culture medium containing 100 μl of a 5 mg/ml 3-(4,5-dimethylthiazol-2-yl)-2,5-diphenyltetrazolium bromide (MTT) solution, followed by 4 h incubation. Next, the MTT-containing medium was replaced with 200 μl isopropanol-HCl (0.1 M), keeping it at 37°C for 10 min to solubilize the formazan crystals. The sample solution was transferred to each well of a 96-well cell-culture plate (Corning) and the absorbance was measured at a wavelength of 570 nm. The percent cell viability of the control (non-treated) cells was taken as 100%.

Statistical analysis

All the data were expressed as the mean ± standard deviation of the mean. Statistical analysis was performed based on the unpaired Student's t-test (two-tailed) and significance was accepted at $P < 0.05$.

RESULTS

Preparation and characterization of cationized gelatin with different amine compounds

Table 1 shows the cationization extent of gelatin samples prepared through the chemical introduction of different amine compounds. The cationization extent could be controlled by changing the molar ratio of amine compounds added. GPC measurement revealed that the molecular weight of all the cationized gelatins used was approximately 1×10^5, irrespective of the type of amine groups introduced.

Table 1.
Cationization extent of gelatin prepared at different molar ratios of amine compounds added to the carboxyl groups of gelatin

Gelatin (g/ml)	Molar ratio[a]	Amino compound (mol%/mol%)[b]			
		Ethylenediamine	Putrescine	Spermidine	Spermine
2×10^{-2}	1	10.4 ± 1.2	11.5 ± 1.0	12.5 ± 1.1	14.1 ± 0.6
2×10^{-2}	10	33.0 ± 1.1	29.6 ± 1.0	32.6 ± 1.2	34.0 ± 1.3
2×10^{-2}	25	42.6 ± 0.8	40.9 ± 1.2	47.6 ± 1.1	47.0 ± 1.2
2×10^{-2}	50	50.9 ± 1.1	45.9 ± 1.0	48.1 ± 1.0	49.0 ± 1.1
2×10^{-2}	100	50.2 ± 1.5	49.8 ± 1.1	54.1 ± 1.3	55.6 ± 1.2

Values are mean ± SD.

[a] The molar ratio of ethylenediamine, putrescine, spermidine and spermine added to the carboxyl groups of gelatin.

[b] The molar percentage of amino residues introduced to the carboxyl groups of gelatin.

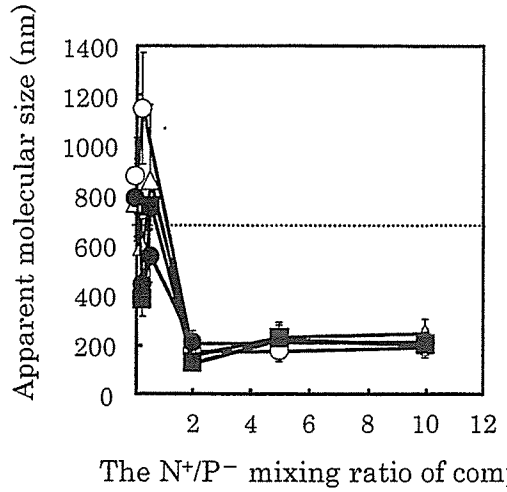

Figure 1. The apparent molecular size of cationized-gelatin–plasmid DNA complexes prepared at different mixing N^+/P^- mixing ratios (the molar number ratio of amino groups of gelatin to the phosphate groups of DNA). The amine compound used for gelatin cationization is ethylenediamine (○), putrescine (△), spermidine (■) and spermine (●). A dotted line indicates the apparent molecular size of naked plasmid DNA.

Our preliminary study revealed that the gene expression level of cationized gelatin-plasmid DNA complexes depended on the cationization extent. Based on this result, the cationization extent of 50 was used for the following experiments unless mentioned otherwise.

Figure 1 shows the apparent molecular size of cationized gelatin-plasmid DNA complexes prepared at different N^+/P^- mixing ratios. The apparent molecular size of plasmid DNA decreased by mixing with the cationized gelatin to around 200 nm, irrespective of the amine compounds introduced, when the N^+/P^- mixing ratio was 1 or higher. The apparent molecular size did not depend on the measurement angle. The zeta potential of cationized gelatin-plasmid DNA complexes prepared at different N^+/P^- mixing ratios tended to increase with increasing the N^+/P^- mixing ratio to obtain a certain zeta potential at the ratio of 2.0, irrespective of the cationized gelatin type (Fig. 2).

Figure 3 shows the electrophoretic patterns of cationized-gelatin–plasmid DNA complexes prepared at different mixing N^+/P^- mixing ratios. The band of plasmid DNA did not migrate for every type of cationized gelatin at the N^+/P^- mixing ratio of 1 or higher. However, the plasmid DNA band was migrated similarly to the original plasmid DNA at N^+/P^- mixing ratios of 0.5 or lower.

Figure 4 shows the fluorescence assay results of EtBr intercalation for various cationized-gelatin–plasmid DNA complexes in aqueous solution. At N^+/P^- mixing ratios of 1 or higher, a significant decrease in the percent fluorescent intensity was detected, irrespective of the cationized gelatin type. In addition, the percentage was significantly lower for the cationized gelatin of spermidine or spermine compared to ethylenediamine or putrescine.

Table 2 shows the K_d values of interaction between the plasmid DNA and various cationized gelatin. The K_d value for the cationized gelatin of spermine

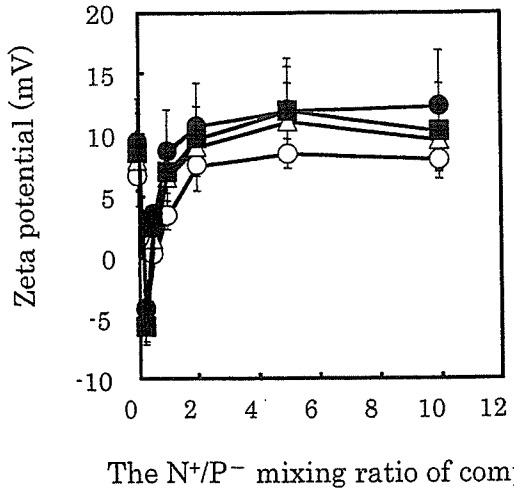

Figure 2. The zeta potential of cationized-gelatin–plasmid DNA complexes prepared at different mixing N^+/P^- mixing ratios (the molar number ratio of amino groups of gelatin to the phosphate groups of DNA). The amine compound used for gelatin cationization is ethylenediamine (○), putrescine (△), spermidine (■) and spermine (●). The zeta potential of naked plasmid DNA is -14.0 ± 2.2 mV.

was 6.4 μM, which is about 6- and 3-times lower than that of putrescine (41 μM) and ethylenediamine (20 μM), respectively.

In vitro *gene expression in L929 cells by various cationized gelatins*

Figure 5 shows the expression level of luciferase for L929 cells cultured with cationized gelatin-plasmid DNA prepared at various N^+/P^- mixing ratios. Three cationized gelatins of spermine showed higher transfection efficiency than that of other amine compounds. In addition, when the cationized gelatin of spermine was used to complex with the plasmid DNA at a N^+/P^- mixing ratio of 2, the highest transfection was achieved. However, no effect of transfection level on the N^+/P^- mixing ratio was observed for the complexes prepared from the cationized gelatin of ethylenediamine, putrescine or spermidine. Based on this result, the N^+/P^- mixing ratio was fixed at 2 for the following gene-transfection experiments. When Lipofectamine was used for transfection of plasmid DNA, the highest luciferase activity observed was 4.87×10^6 RLU/mg protein, which is significantly lower compared with that of any cationized gelatin.

Figure 6 shows the effect of N^+/P^- mixing ratio on the cytotoxicity of cationized gelatin-plasmid DNA complexes for L929 cells. Cell toxicity was observed for every complex when the N^+/P^- mixing ratio was 5 or higher, although it tended to be higher for the cationized gelatin of spermine compared with that of other cationized gelatins. When Lipofectamine was used for transfection of the plasmid DNA, the viability of cells was $72.1 \pm 5.2\%$, which is significantly higher compared with that of any cationized gelatin.

Figure 7 shows the effect of the cell density on the gene transfection of cationized gelatin derivatized with spermine–luciferase–plasmid DNA complexes for L929

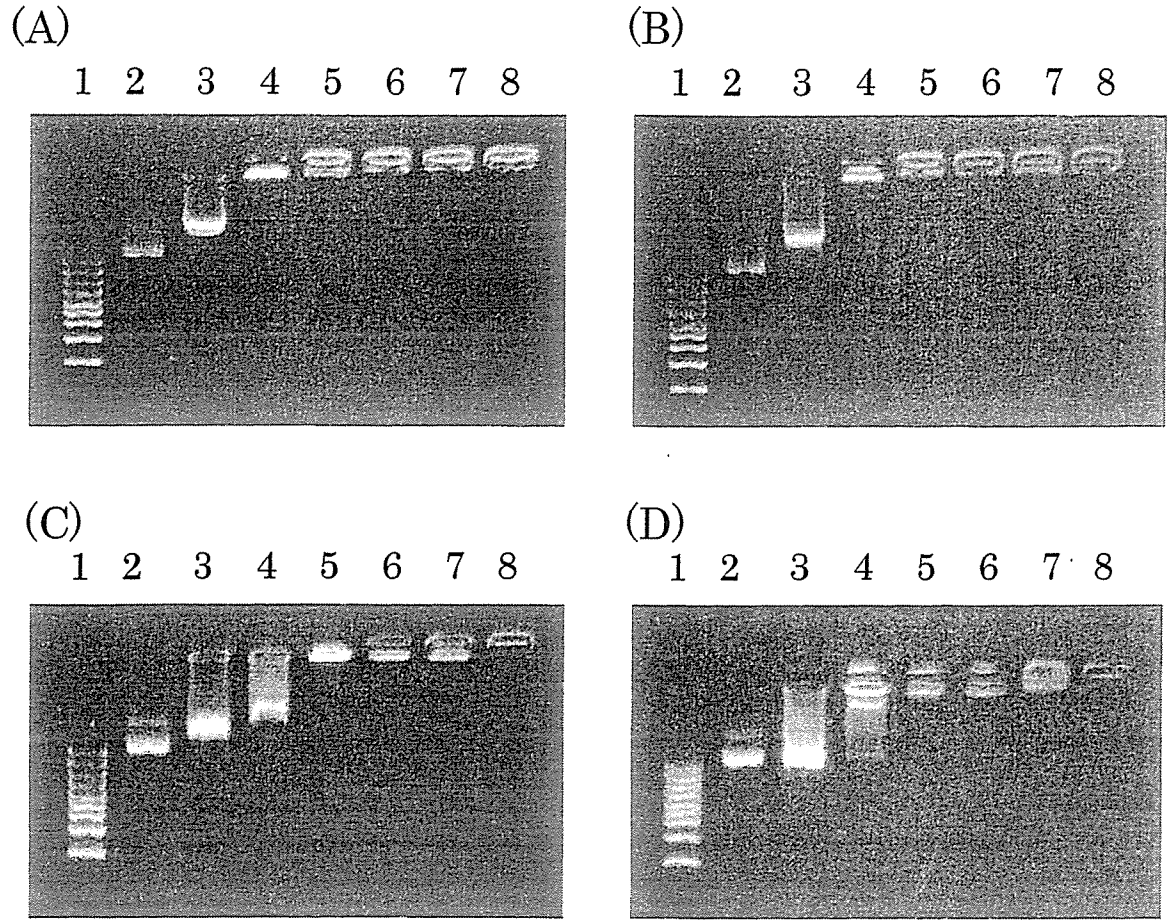

Figure 3. Electrophoretic patterns of cationized-gelatin–plasmid DNA complexes prepared at different mixing N^+/P^- mixing ratios (the molar number ratio of amino groups of gelatin to the phosphate groups of DNA). Lane 1, molecular marker; lane 2, naked plasmid DNA; lanes 3–8, plasmid DNA complexed with the cationized gelatin at N^+/P^- mixing ratios (the molar number ratio of amino groups of gelatin to the phosphate groups of DNA) of 0.25, 0.5, 1, 2, 5 and 10, respectively. The amine compound used for gelatin cationization was (A) ethylenediamine, (B) putrescine, (C) spermidine and (D) spermine.

cells. The highest gene expression level was observed at a cell seeding density of 2.5×10^4 cells/well.

DISCUSSION

In the present study, the efficacy of cationized gelatin prepared from different amine compounds as a non-viral gene delivery system was evaluated.

The cationized-gelatin–plasmid DNA complex showed an apparent molecular size in the nanometer range (Fig. 1). The complex size was around 200 nm when the N^+/P^- mixing ratio was over 1, irrespective of the type of amine compound used. It has been demonstrated that the complex with this size range can be favorably taken up by cells [29, 30]. This is also an advantageous feature of the plasmid DNA complex prepared from the cationized gelatin to enhance the transfection efficiency

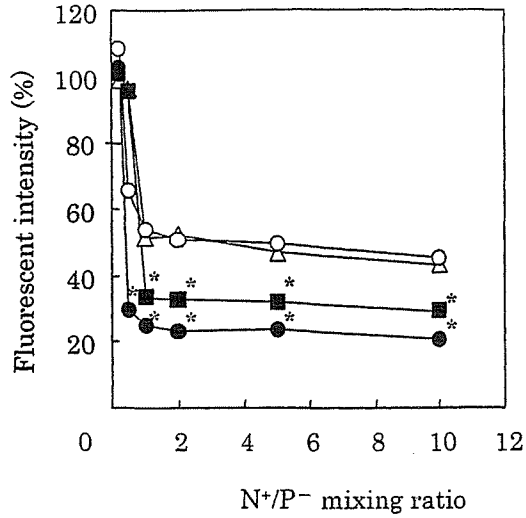

Figure 4. EtBr intercalation fluorescence assay for various cationized-gelatin–plasmid DNA complexes in aqueous solution. The fluorescence of EtBr intercalated into plasmid DNA was exclusively detected. The amine compound used for gelatin cationization is ethylenediamine (○), putrescine (△), spermidine (■) and spermine (●). The fluorescent intensity of EtBr intercalated to free plasmid DNA is defined as 100% for relative fluorescence. $*P < 0.05$, significant difference in the fluorescent intensity against the cationized gelatin prepared from ethylenediamine.

Table 2.
The K_d values of the interaction between plasmid DNA and the cationized gelatins

Amino compound	Temperature (°C)	K_d (μM)	Cationized-gelatin–plasmid DNA binding capacity (mol/mol)
Ethylenediamine	37	20.4	487.9
Putrescine	37	40.5	346.8
Spermidine	37	4.59	240.8
Spermine	37	6.35	210.4

The molar ratio of amino compound added to the carboxyl groups of gelatin was 100.

for gene expression in terms of efficient DNA condensing to a nano-order size. In addition, the surface charge of cationized-gelatin–plasmid DNA complex was tended to increase with increasing N^+/P^- mixing ratio (Fig. 2). These findings strongly suggest that the cationized-gelatin–plasmid DNA complex has a nano-size structure of which surface is covered with cationized gelatin molecules.

The gel retardation assay revealed that the cationized gelatin electrostatically interacted with the plasmid DNA. With an increase in the N^+/P^- mixing ratio, the plasmid DNA band did not migrate in electrophoresis (Fig. 3). It is possible that the negative charge of plasmid DNA is neutralized by complexation with the cationized gelatin and the molecular size of plasmid DNA increases with the cationized gelatin complexation, resulting in reduced electrophoretic migration of plasmid DNA. From the EtBr intercalation assay, relative fluorescence percentage of the complex from cationized gelatin prepared from ethylenediamine or putrescine was larger than that of spermidine or spermine (Fig. 4). The cationized gelatin prepared from

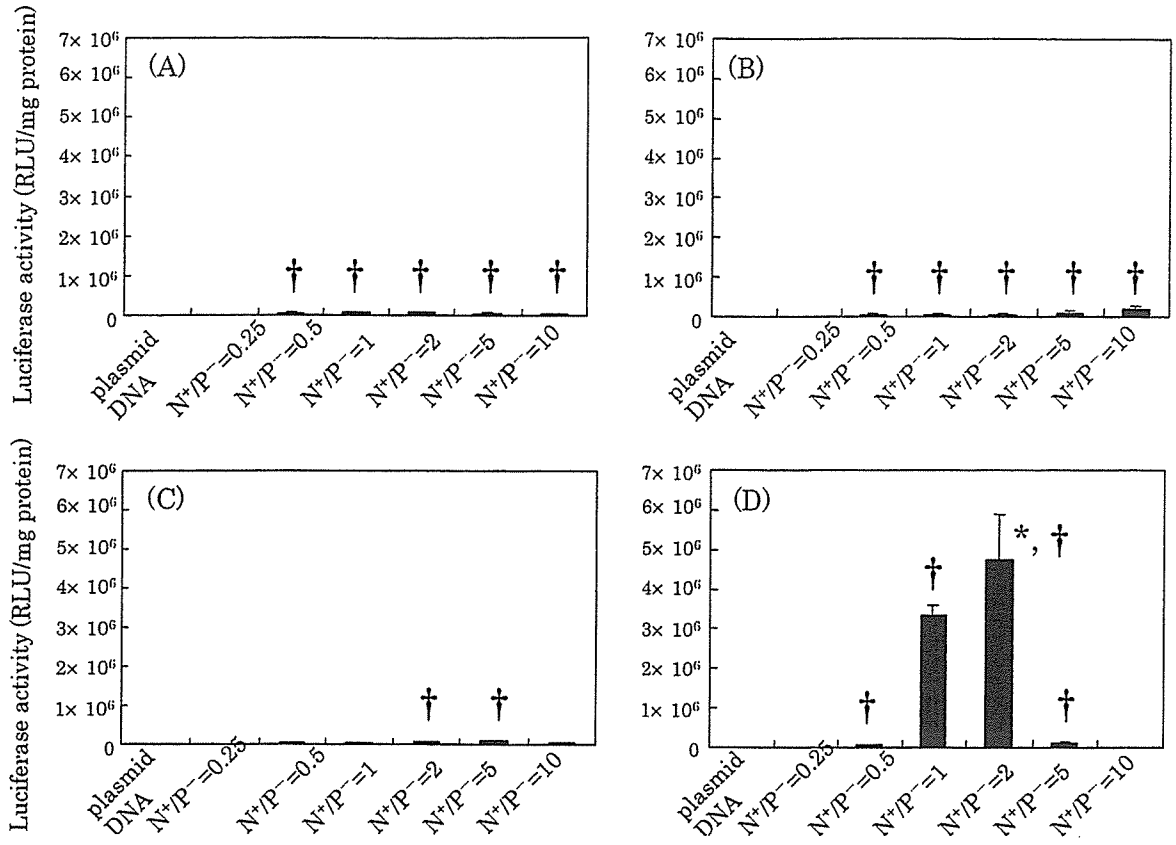

Figure 5. Effect of N^+/P^- mixing ratio (the molar number ratio of amino groups of gelatin to the phosphate groups of DNA) on the luciferase activity of L929 cells transfected by cationized-gelatins–luciferase–plasmid DNA complexes. The amine compound used for gelatin cationization was (A) ethylenediamine, (B) putrescine, (C) spermidine and (D) spermine. $^*P < 0.05$, significant difference in the luciferase activity against the complexes prepared at other N^+/P^- mixing ratios; $^\dagger P < 0.05$, significant difference in the luciferase activity against free plasmid DNA.

ethylenediamine or putrescine was intercalated about 2-fold more easily by EtBr than that of spermidine or spermine at a N^+/P^- mixing ratio of 2, indicating that the affinity of the cationized gelatin prepared from ethylenediamine or putrescine for the plasmid DNA was explicitly smaller than that of spermidine or spermine. For cationic polymers, it is conceivable that electrostatic interaction with the plasmid DNA inhibits the EtBr intercalation, resulting in a large decrease in the fluorescence intensity. The Scatchard plot analysis also demonstrates that the interaction of plasmid DNA with the cationized gelatin derivatized with ethylenediamine or putrescine was weaker than that with spermidine or spermine (Table 2). This experimentally supports the result of EtBr intercalation assay.

The transfection conditions of plasmid-DNA–cationized gelatin complexes for L929 cells, such as N^+/P^- mixing ratio, the cytotoxicity and the cell density, were optimized (Figs 5–7). From these results, the cationized gelatin prepared from spermine was suitable to obtain high transfection efficiency at a N^+/P^- mixing ratio of 2 and cell density of 70%. In addition, the cationized gelatin prepared from spermine showed a large EtBr fluorescence decrease compared with that of

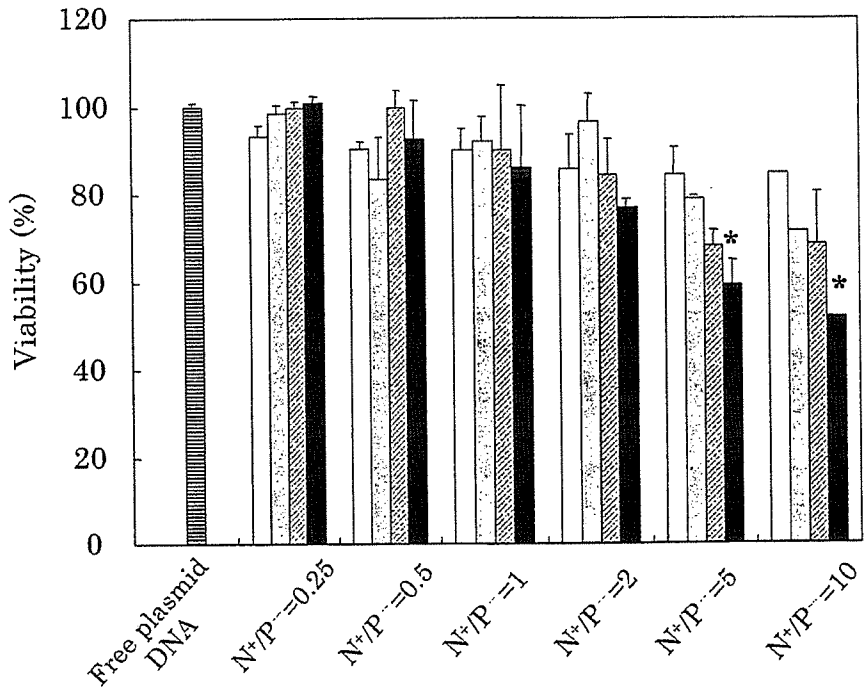

Figure 6. Effect of the N^+/P^- mixing ratio (the molar number ratio of amino groups of gelatin to the phosphate groups of DNA) on the cytotoxicity of L929 cells incubated with cationized-gelatin–luciferase–plasmid DNA complexes. The amine compound used for gelatin cationization was ethylenediamine (□), putrescine (▩), spermidine (▨) and spermine (■).

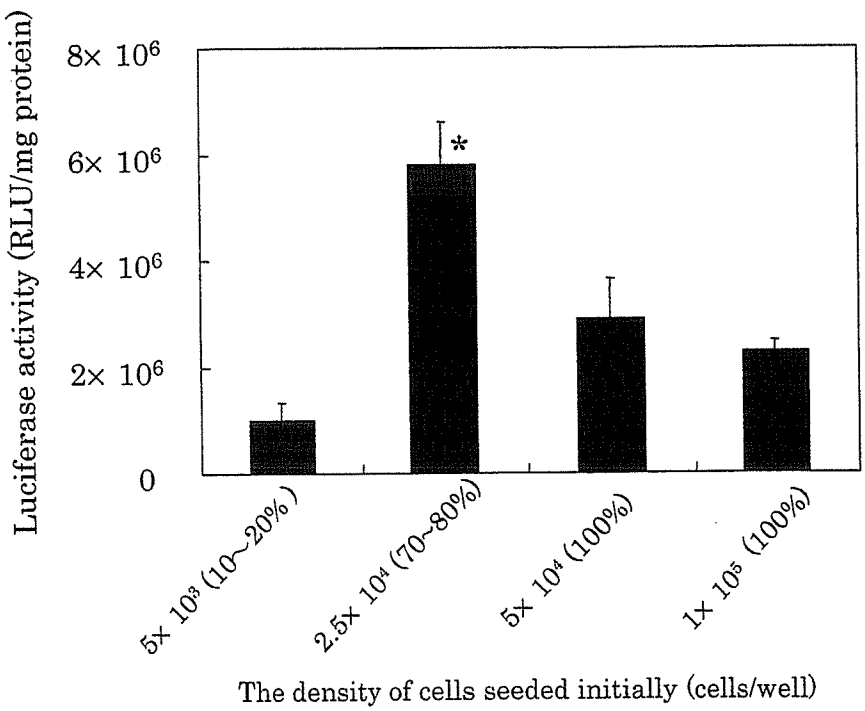

Figure 7. Effect of the cell density on the gene expression of the cationized gelatin derivatized with spermine–luciferase plasmid DNA complex prepared at a N^+/P^- mixing ratio of 2 for L929 cells. Cells were cultured for 24 h before complex addition, while the apparent cell confluency is indicated as the number in parentheses. $^*P < 0.05$, significant difference in the luciferase activity against other groups at the corresponding N^+/P^- mixing ratio.

other amine compounds (Fig. 4). The lowest intensity for the cationized gelatin prepared from spermine was observed at a N^+/P^- mixing ratio of 2, indicating the sufficiently interaction with the DNA. The luciferase expression enhancement was higher for the cationized gelatin prepared from spermine than that of other amine compounds (Fig. 5). This can be explained in terms of the buffering capacity of complexes in addition to their molecular size and charge. Our previous study with the same four types of cationized gelatins revealed that the cationized gelatin prepared from spermine possessed the highest buffering effect among all the cationized gelatins used [31]. Both the condensed structure and a net positive charge of cationized-polymer–plasmid DNA complexes have been reported to be key for gene transfection [32]. However, as the N^+/P^- mixing ratio of cationized gelatin prepared from spermine increased, the viability of transfected cells decreased (Fig. 6). There was no difference in the molecular size and charge of complexes between the cationized gelatins of spermine and other amines (Figs 1 and 2). The reason of higher cytotoxicity for spermine-introduced cationized gelatin is not clear at present.

In conclusion, the plasmid DNA was complexed with cationized gelatin prepared from spermine and the *in vitro* expression level of plasmid DNA complexed increased significantly compared with that prepared from other amine compounds at optimal conditions determined. Plasmid DNA is a macromolecule with a negative charge, irrespective of the type of the coded protein. Therefore, it is practically possible to think of the plasmid DNA as one type of biological substance with the similar nature of charge, an anionic macromolecule. This cationized gelatin is being applied as the non-viral carrier for the plasmid DNA of bioactive molecules like growth factor to demonstrate enhancement of the *ex vivo* biological functions at present.

REFERENCES

1. J. Bonadio, E. Smiley, P. Patil and S. Goldstein, *Nature Med.* **5**, 753 (1999).
2. M. F. Pittenger, A. M. Mackay, S. C. Beck, R. K. Jaiswal, R. Douglas, J. D. Mosca, M. A. Moorman, D. W. Simonetti, S. Craig and D. R. Marshak, *Science* **284**, 143 (1999).
3. S. Wakitani, T. Saito and A. I. Caplan, *Muscle Nerve* **18**, 1417 (1995).
4. D. Woodbury, E. J. Schwarz, D. J. Prockop and I. B. Black, *J. Neurosci. Res.* **61**, 364 (2000).
5. M. Reyes, T. Lund, T. Lenvik, D. Aguiar, L. Koodie and C. M. Verfaillie, *Blood* **98**, 2615 (2001).
6. E. M. Horwitz, D. J. Prockop, L. A. Fitzpatrick, W. W. Koo, P. L. Gordon, M. Neel, M. Sussman, P. Orchard, J. C. Marx, R. E. Pyeritz and M. K. Brenner, *Nature Med.* **5**, 309 (1999).
7. R. F. Pereira, K. W. Halford, M. D. O'Hara, D. B. Leeper, B. P. Sokolov, M. D. Pollard, O. Bagasra and D. J. Prockop, *Proc. Natl. Acad. Sci. USA* **92**, 4857 (1995).
8. E. M. Horwitz, P. L. Gordon, W. K. Koo, J. C. Marx, M. D. Neel, R. Y. McNall, L. Muul and T. Hofmann, *Proc. Natl. Acad. Sci. USA* **99**, 8932 (2002).
9. T. J. Oligino, Q. Yao, S. C. Ghivizzani and P. Robbins, *Clin. Orthoped.* **379**, S17 (2000).
10. O. Zelphati, C. Nguyen, M. Ferrari, J. Felgner, Y. Tsai and P. L. Felgner, *Gene Ther.* **5**, 1272 (1998).

11. I. K. Park, T. H. Kim, Y. H. Park, B. A. Shin, E. S. Choi, E. H. Chowdhury, T. Akaike and C. S. Cho, *J. Control. Rel.* **76**, 349 (2001).
12. X. Gao and L. Huang, *Biochemistry* **35**, 1027 (1996).
13. N. J. Caplen, E. W. Alton, P. G. Middleton, J. R. Dorin, B. J. Stevenson, X. Gao, S. R. Durham, P. K. Jeffery, M. E. Hodson and C. Coutelle, *Nature Med.* **1**, 39 (1995).
14. M. Cotton and E. Wagner, *Curr. Opin. Biotechnol.* **4**, 705 (1993).
15. A. V. Kabanov and V. A. Kabanov, *Bioconj. Chem.* **6**, 7 (1995).
16. S. Han, R. I. Mahato, Y. K. Sung and S. W. Kim, *Mol. Ther.* **2**, 302 (2000).
17. A. Veis, *Int. Rev. Connect. Tissue Res.* **3**, 113 (1965).
18. T. Kushibiki, R. Tomoshige, Y. Fukunaka, M. Kakemi and Y. Tabata, *J. Control. Rel.* **90**, 207 (2003).
19. Y. Fukunaka, K. Iwanaga, K. Morimoto, M. Kakemi and Y. Tabata, *J. Control. Rel.* **80**, 333 (2001).
20. T. Kushibiki and Y. Tabata, *Curr. Drug Deliv.* **1**, 153 (2004).
21. T. Kushibiki, K. Matsumoto, T. Nakamura and Y. Tabata, *Gene Ther.* **11**, 1205 (2004).
22. T. Kushibiki, K. Matsumoto, T. Nakamura and Y. Tabata, *Pharm. Res.* **21**, 1109 (2004).
23. S. L. Snyder and P. Z. Sobocinski, *Anal. Biochem.* **64**, 284 (1975).
24. D. Fischer, T. Bieber, Y. Li, H. P. Elsaesser and T. Kissel, *Pharm. Res.* **16**, 1273 (1999).
25. Y. Xu and F. C. Szoka Jr., *Biochemistry* **35**, 5616 (1996).
26. H. C. Chan, W. T. Ruyechan and J. G. Wetmur, *Biochemistry* **15**, 5487 (1976).
27. G. Scatchard, *Ann. NY. Acad. Sci.* **51**, 660 (1949).
28. D. P. Lennon, S. E. Haynesworth, R. G. Young, J. E. Dennis and A. I. Caplan, *Exp. Cell Res.* **219**, 211 (1995).
29. W. Zauner, A. Kichler, W. Schmidt, A. Sinski and E. Wagner, *Biotechniques* **20**, 905 (1996).
30. P. Midoux and M. Monsigny, *Bioconj. Chem.* **10**, 406 (1999).
31. H. Hosseinkhani and Y. Tabata, *J. Control. Rel.* **86**, 169 (2003).
32. B. Abdallah, L. Sachs and B. A. Demeneix, *Biol. Cell* **85**, 1 (1995).

Characterization of DNA release from composites of oligo(poly(ethylene glycol) fumarate) and cationized gelatin microspheres *in vitro*

F. Kurtis Kasper,[1] Erin Jerkins,[1] Kazuhiro Tanahashi,[1] Michael A. Barry,[1,2] Yasuhiko Tabata,[3] Antonios G. Mikos[1]

[1]*Department of Bioengineering, Rice University, PO Box 1892, MS-142, Houston, Texas 77251-1892*
[2]*Center for Cell and Gene Therapy, Baylor College of Medicine, One Baylor Plaza, N1002, Houston, Texas 77030*
[3]*Department of Biomaterials, Institute for Frontier Medical Sciences, Kyoto University, 53 Kawara-cho, Shogoin, Sakyo-ku, Kyoto 606-8507, Japan*

Received 14 September 2005; revised 23 November 2005; accepted 20 January 2006
Published online 1 June 2006 in Wiley InterScience (www.interscience.wiley.com). DOI: 10.1002/jbm.a.30736

Abstract: This research investigates the release of plasmid DNA from novel hydrogel composites of oligo(poly(ethylene glycol) fumarate) (OPF) and cationized gelatin microspheres (CGMS), as well as the swelling and degradation of these materials *in vitro*. The release of total DNA and of double-stranded DNA was measured fluorescently, and the swelling properties and polymer mass loss of the hydrogels were assessed. Further, the structural integrity of the released DNA was determined through electrophoresis. It was found that plasmid DNA can be released in a sustained fashion over the course of up to 49–140 days *in vitro* from hydrogels of OPF synthesized from poly(ethylene glycol) of nominal molecular weights of 10 kDa and 3 kDa, respectively, with the release kinetics depending upon the material composition and the method of DNA loading. Released DNA was predominately double-stranded DNA (dsDNA) in structure and of the open-circular conformation. The results suggest that DNA release from hydrogel composites of OPF and CGMS is dominated by the degradation of the OPF component of the gels. Electrophoresis results indicate that the released DNA retains suitable conformation for potential bioactivity over the course of at least 63 days of release. Thus, these studies demonstrate the potential of composites of OPF and CGMS in controlled gene delivery applications.
 J Biomed Mater Res 78A: 823–835, 2006

Key words: controlled release; degradable hydrogel; gelatin microspheres; plasmid DNA; tissue engineering

INTRODUCTION

Tissue engineering strategies for regeneration of compromised tissues generally comprise a scaffold, cells, and/or bioactive molecules. Employment of a scaffold material is often necessary to provide support and guidance to the growing tissue. Additionally, cells and/or bioactive molecules may be used in conjunction with a scaffold to direct tissue development toward a desired pathway. Although therapeutic proteins may be delivered with and released from tissue engineering scaffolds, it has been proposed that the instability of the proteins themselves raises the greatest concern regarding the success of these systems for long-term (days to months) controlled release.[1]

However, the delivery of plasmid DNA encoding a therapeutic protein presents a promising alternative to the outright delivery of the protein. Indeed, the chemical stability of plasmid DNA facilitates the application of traditional methods established for the controlled release of proteins toward achieving controlled gene delivery.[2] The success of therapeutic gene delivery from a tissue engineering scaffold, however, requires a system that provides control of DNA release, facilitates cellular uptake of DNA, maintains gene expression, and provides support for tissue infiltration while presenting void volume into which tissue may grow.

Although many materials have been explored toward application in the controlled release of plasmid DNA, cationized gelatin has been demonstrated to allow for prolonged and enhanced gene expression *in vivo*, relative to injected plasmid DNA solution.[3–6] A

Correspondence to: A. G. Mikos; e-mail: mikos@rice.edu
Contract grant sponsor: National Institutes of Health; contract grant number: R01 DE15164
Contract grant sponsor: NSF-IGERT; contract grant number: DGE-0114264

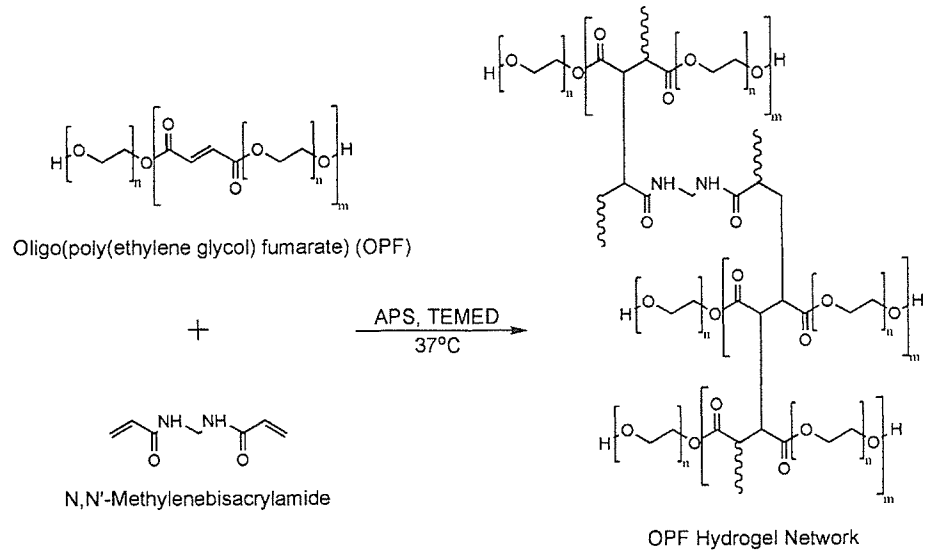

Figure 1. Schematic of the crosslinking reaction that occurs with OPF and *N,N'*-methylenebisacrylamide, using the water soluble initiator system APS/TEMED.

primary advantage presented by cationized gelatin in DNA release applications is the formation of electrostatic complexes between the material and plasmid DNA,[4,7,8] such that the DNA is electrostatically bound to the cationized gelatin upon loading.[3] Thus, the release of plasmid DNA from hydrogels and microspheres created from cationized gelatin is driven by the enzymatic degradation of the cationized gelatin, the kinetics of which may be controlled through the crosslinking extent of the cationized gelatin.[3–6] Upon release, the DNA likely remains complexed with degradation fragments of the cationized gelatin.[3] It has been proposed that this complexation may reduce degradation of the DNA by nucleases and may facilitate cellular entry through interaction of the positively charged complexes with negatively charged cell membranes.[4] Thus, hydrogels and microspheres of cationized gelatin are attractive and effective materials for controlled gene delivery.

However, the duration of plasmid DNA release from cationized gelatin hydrogels and microspheres is limited by the enzymatic degradation of the cationized gelatin network. In the case of cationized gelatin microspheres, the observed release of plasmid DNA has generally been limited to ~3–4 weeks *in vivo*.[5,9] Applications for therapeutic gene delivery and tissue engineering, however, often call for sustained protein expression, which may require the persistence of DNA beyond a few weeks. Additionally, tissue engineering applications require the presence of a scaffold material for a period of time sufficient to support tissue growth.

A potential method to retain the benefits provided by cationized gelatin, while extending the duration of the release of DNA and the persistence of the scaffold, may be found in the formation of composites of cationized gelatin microspheres with another material, such as oligo(poly(ethylene glycol) fumarate) (OPF) (Fig. 1). OPF is a water-soluble material that can be crosslinked in situ under physiological conditions to form hydrogels, which have been demonstrated to be biocompatible and biodegradable[10,11] and have been applied toward cell attachment,[12–14] cell encapsulation,[15,16] and controlled release of plasmid DNA.[17,18] Indeed, composites of OPF and CGMS have been shown to extend the release of plasmid DNA *in vivo* relative to DNA release from CGMS alone.[18] Control of the release of plasmid DNA from the composites appeared to be dominated by the degradation of the OPF network.[18] However, the determination of the degradation kinetics of the OPF was not explored in the previous investigation.[18] Thus, the present work seeks to expand upon prior work to advance the understanding of DNA release from composites of OPF and CGMS.

The objectives of the present study were to characterize the release of plasmid DNA *in vitro* from composites of OPF and CGMS and from control hydrogels of OPF alone. As a part of the study, the release of plasmid DNA from the OPF phase and from the CGMS phase of composites was examined individually to directly assess the effect of the manner of DNA loading upon DNA release, thereby giving an indirect evaluation of the effect of potential electrostatic complexation between the DNA and CGMS upon DNA release. Additionally, the present work sought to characterize the swelling and degradation of these hydrogels *in vitro*.

MATERIALS AND METHODS

Plasmid DNA preparation

The expression vector encoding human Bone Morphogenetic Protein-2 (hBMP-2) with an upstream CMV promoter (pCMV-hBMP2, 4.9 kb) was prepared from *Escherichia coli* (*E. coli*) bacterial cultures with a QIAfilter Plasmid Giga Kit (Qiagen, Valencia, CA) according to the manufacturer's protocol. The isolated plasmid DNA was dissolved in a small volume of TE buffer (10 m*M* Tris HCl; 1 m*M* EDTA, pH 7.5). The concentration of plasmid DNA in solution was determined from the UV absorbance at a wavelength of 260 nm (A_{260}), and the ratio of the absorbance at wavelengths of 260 and 280 nm (A_{260}/A_{280}) was measured for evaluation of plasmid purity to be between 1.8 and 2.0.

Hydrogel composite fabrication

OPF was synthesized and characterized according to established methods[19] from PEG of a nominal molecular weight of either 3K (Union Carbide, New Milford, CT) or 10K (Sigma-Aldrich, St. Louis, MO) and termed "OPF 3K" and "OPF 10K," respectively. Porcine gelatin with an isoelectric point of 9.0 (MW 100,000) (Nitta Gelatin, Osaka, Japan) was cationized through the introduction of amino groups by chemical conversion of carboxyl groups of the gelatin as previously described.[3–5] Cationized gelatin microspheres (CGMS) were prepared through the chemical crosslinking of cationized gelatin in a water-in-oil emulsion state,[20] using a 6 m*M* glutaraldehyde concentration as described previously.[18] The CGMS were fractionated in size by sieves to obtain microspheres in the range of 30–90 μm in diameter.

OPF constructs and composites of OPF and CGMS with and without incorporated plasmid DNA were prepared as previously described.[18] First, OPF (300 mg) was dissolved in 790 μL of phosphate buffered saline (PBS) (4 m*M* KH_2PO_4; 18 m*M* $Na_2HPO_4 \cdot 12\ H_2O$; 125 m*M* NaCl; pH 7.4) containing 28 mg *N,N'*-methylene bisacrylamide as a crosslinking agent. Second, for composite samples in which DNA was to be loaded into the CGMS component, freeze-dried CGMS (4 mg) were reconstituted through incubation overnight at 4°C with 40 μL of PBS/DNA solution, a volume less than the known equilibrium swelling volume, to load the CGMS with DNA. Similarly, for composite samples in which the CGMS were not to contain DNA, freeze-dried CGMS (4 mg) were reconstituted through incubation at 4°C overnight with 40 μL of PBS. For composite samples in which the DNA was to be loaded into the OPF component, 196 μL of PBS and 40 μL of PBS/DNA solution were then added, along with the blank CGMS, into the OPF polymer solution. For composite samples in which the DNA was to be loaded in the CGMS component, 236 μL of PBS were added, along with the DNA-loaded CGMS, into the OPF polymer solution. In both cases, the resulting polymer solutions were vigorously mixed to disperse the microspheres in the solution. For OPF samples without a CGMS component, either 236 μL of PBS (for blank samples) or 196 μL of PBS and 40 μL of PBS/DNA solution (for DNA loaded samples) were added to the OPF polymer solution and mixed. In this way, for samples in which DNA was to be loaded into OPF, the DNA was incorporated into and dispersed throughout the OPF polymer solution prior to the formation of the crosslinked hydrogel network. Third, 102 μL of 0.3*M* tetramethylethylenediamine (TEMED) (in PBS) and 102 μL of 0.3*M* ammonium persulfate (APS) (in PBS) were added to the polymer solution and thoroughly mixed to disperse the microspheres (if present in that sample type) and initiate crosslinking of the network. Immediately after mixing, the suspension was injected into individual wells (8 mm diameter, 2 mm height) of a Teflon mold and incubated at 37°C to facilitate crosslinking of the polymer network. After 30 min, the hydrogel networks were removed from the mold, yielding discs of ~8 mm diameter and 2 mm thickness.

In vitro DNA release

Hydrogel samples were placed individually into separate containers containing 3 mL of PBS (pH 7.4) with 373 ng/mL bacterial collagenase 1A (Sigma-Aldrich, St. Louis, MO). The presence of collagenase in solution was necessary for enzymatic degradation of the CGMS, and it was incorporated into the PBS at a concentration that approximates physiologically relevant concentrations.[21] The specimens were agitated on a shaker at ~70 rpm at 37°C for the duration of the study. The release solution was completely removed from the samples and replaced with fresh solution at periodic time points.

The amount of DNA in the release solution aliquots was quantified through a fluorescent method with PicoGreen dsDNA Quantitation Reagent (Molecular Probes, Eugene, OR) and OliGreen ssDNA Quantitation Reagent (Molecular Probes, Eugene, OR) termed PicoGreen and OliGreen, respectively, according to the manufacturer's guidelines. Briefly, for each assay, 100 μL of each sample release solution was added independently to individual wells in an opaque 96-well plate. Then 50 μL of TE buffer was added to each well. A 200-fold dilution of the respective reagent was prepared in TE buffer, and 150 μL of the diluted reagent was added to each well. After a 10-min equilibration period, the fluorescence intensity of each well was measured with a microplate fluorescence reader (FLx800, BIO-TEK Instruments, Winooski, VT) equipped with 480/525 (excitation/emission) filter sets.

Three independent wells were prepared from the release solution of each release specimen at each time point. Five standard solutions of known DNA concentrations were prepared from the DNA stock solution used in the fabrication of the hydrogels. The stock solution was housed with the release samples at 37°C under agitation at ~70 rpm. An aliquot of the stock solution was taken at each time point and was serially diluted in PBS with 373 ng/mL collagenase to form the calibration standards used to analyze the release solutions from the respective time point. The average fluorescence of release solutions from hydrogels not incorporating plasmid DNA was subtracted from the fluorescence values of respective samples with DNA to account for any effects of the polymer on the assay. The cumulative fraction

release for each specimen was normalized with respect to the volumetrically calculated initial DNA content. The sample number, n, for all DNA release groups was 6.

Gel electrophoresis of released DNA

A sample of plasmid DNA released from each hydrogel group was analyzed on 1% wt. agarose gels prepared with 50 mL TAE buffer (40 m*M* Tris-acetate, 1 m*M* EDTA, pH 8.3) and 25 μg ethidium bromide for days 3–63. For each group, released plasmid DNA was isolated from the combined release solution aliquots of the polymer mass loss samples for that group at a given time point, using ethanol precipitation. Briefly, 500 μL ethanol and 20 μL 5*M* NaCl were added to 200 μL of the combined release solution in a microcentrifuge tube. The tube was inverted to mix the solution and spun at 13,000 rpm for 30 min at room temperature. The supernatant was aspirated carefully from the tube, and the DNA pellet was allowed to air dry for ~15 min. The pellet was resuspended in 10 μL TE and 2 μL of 6× agarose gel loading dye was added. Samples of a 1 μg/mL dilution of the DNA standard solution aliquot from each time point (days 3–63) were prepared in the same fashion. Lanes of the gel were loaded with 10 μL of the sample/dye solution. Additionally, a lambda DNA/EcoRI+HindIII marker was run on each gel to allow for comparison of DNA migration distances between gels. All gels were run at 80 V for 60 min in 1× TAE buffer, followed by digital imaging in a UV transillumination box.

Hydrogel swelling and degradation

The initial weight (W_i) of all samples was measured immediately after fabrication, but before the addition of the initial 3 mL of PBS/collagenase solution. Thus, W_i represents the mass of the hydrogel immediately after fabrication and prior to equilibrium swelling. Additionally, the wet weight (W_w) of all release samples and polymer mass loss samples were measured at the pertinent time point immediately upon removal of the release solution. The swelling ratio of the hydrogels at each time point was calculated accordingly from the following equation:

$$\text{Swelling Ratio} = \frac{W_w - W_i}{W_i} \quad (1)$$

This value reflects the change in weight of the hydrogel at each time point with respect to the initial weight of the gel. As a hydrogel degrades, the wet weight of the gel approaches zero. Thus, the value of the swelling ratio approaches a value of −1 upon hydrogel degradation.

The polymer mass loss was calculated for three samples from each group at each time point for days 3–63. Immediately after fabrication, six samples from each group were lyophilized, and the dry polymer mass was measured for each. The average mass of the six samples for each group was calculated and used as the initial dry polymer weight ($W_{i,d}$) for that group in subsequent calculations. At each time point, three samples from each group were lyophilized immediately after aspiration of the release solution, and the dry polymer mass (W_d) was measured for each. The fraction of initial polymer mass remaining for each sample was then calculated from the following equation:

$$\text{Fraction Initial Polymer Mass Remaining} = \frac{W_d}{W_{i,d}} \quad (2)$$

Complete degradation of a hydrogel sample was noted visually when the presence of the disk or fragments of the disk were no longer apparent.

TABLE I
Number Average (M_n) and Weight Average (M_w) Molecular Weight Values of PEG and OPF as Determined by Gel Permeation Chromatography (Each Sample was Run in Triplicate)

	M_n	M_w
PEG 3K	4,000 ± 0,000	5,000 ± 0,000
PEG 10K	12,000 ± 0,000	14,000 ± 0,000
OPF 3K	14,000 ± 1,000	83,000 ± 0,000
OPF 10K	24,000 ± 1,000	63,000 ± 5,000

Statistical analysis

The cumulative fraction release values of plasmid DNA were statistically compared between assay types (OliGreen and PicoGreen) within material formulations (OPF 3K, OPF 10K, and composite groups) as well as between material formulations within an assay type at each time point, using Student's t-test ($p < 0.05$). Similarly, the swelling ratio and polymer mass loss values were statistically compared between loading treatment groups (blank and with DNA) within material formulations (OPF 3K, OPF 10K, and composite groups) as well as between material formulations within loading treatment groups, using Student's t-test ($p < 0.05$). Other statistical comparisons were made as described. Error propagation methods were employed where appropriate to determine standard deviations.[22] All values are reported as average ± standard deviation.

RESULTS

Gel permeation chromatography

The number average and weight average molecular weights of the initial PEG and resulting OPF are reported in Table I for both OPF formulations.

In vitro DNA release

The release of plasmid DNA from OPF hydrogels [Fig. 2(a)] and composites of OPF and CGMS [Fig.

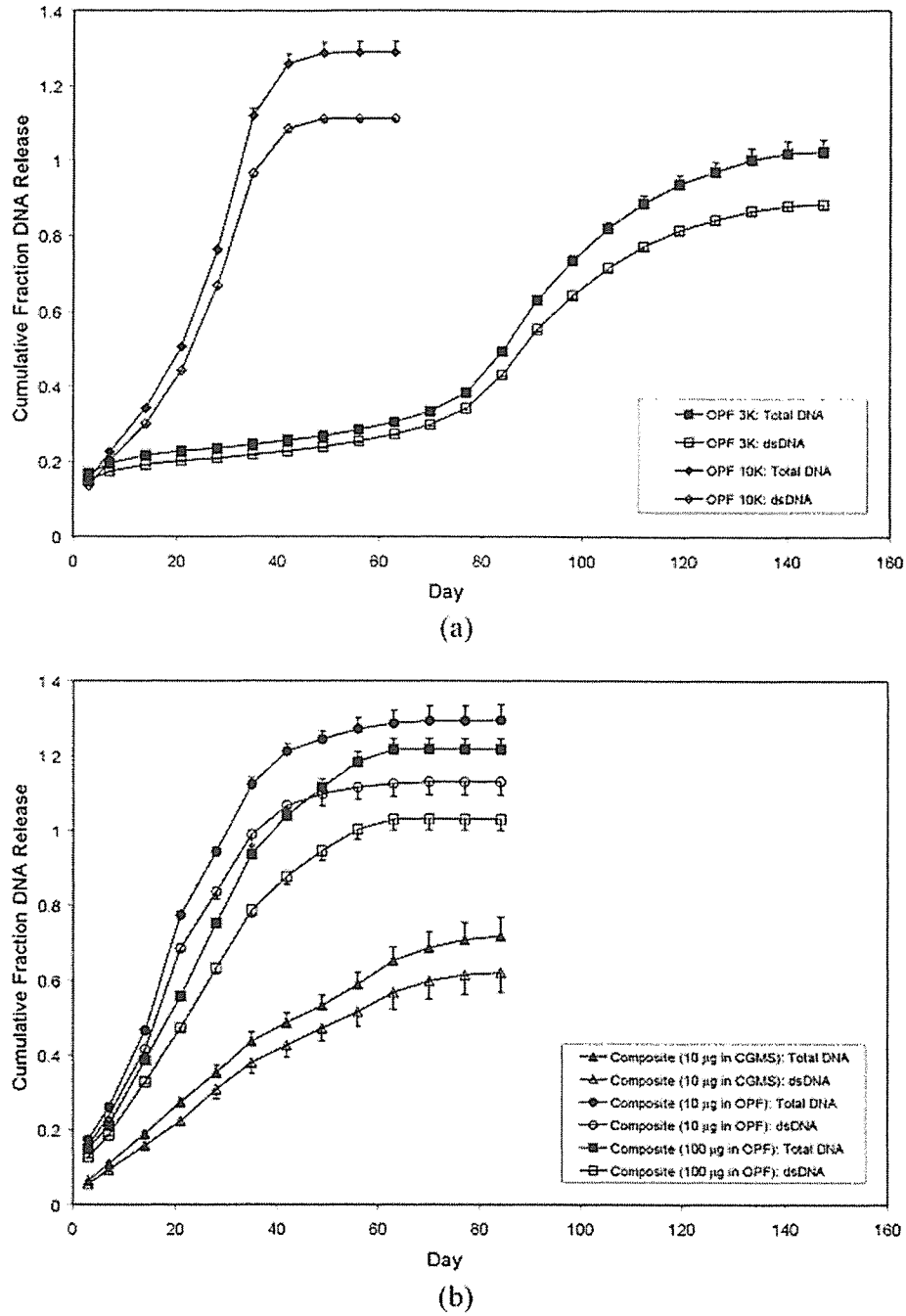

Figure 2. Release profiles of total DNA and double-stranded DNA (dsDNA) from OPF hydrogels (a) and from hydrogel composites of OPF and CGMS (b) in enzymatic PBS (pH 7.4) ($n = 6$). Error bars represent ± standard deviation.

2(b)] occurred in a sustained fashion over the course of up to 49–140 days *in vitro*. The cumulative fraction of DNA released, as determined by OliGreen, increased with time relative to that determined by PicoGreen for each OPF and composite formulation. The cumulative fraction of DNA released, as determined by OliGreen, was significantly higher than that determined by PicoGreen for OPF 3K at days 112–147 ($p < 0.05$). In the case of OPF 10K, the cumulative fraction of DNA released, as determined by OliGreen, was significantly greater than that quantified by PicoGreen at days 3 and 42–63 ($p < 0.05$). Similarly, for composite groups in which DNA was loaded into the OPF component, the cumulative fraction of DNA released, as determined by OliGreen, was significantly higher than the value determined by PicoGreen at days 42–84 and

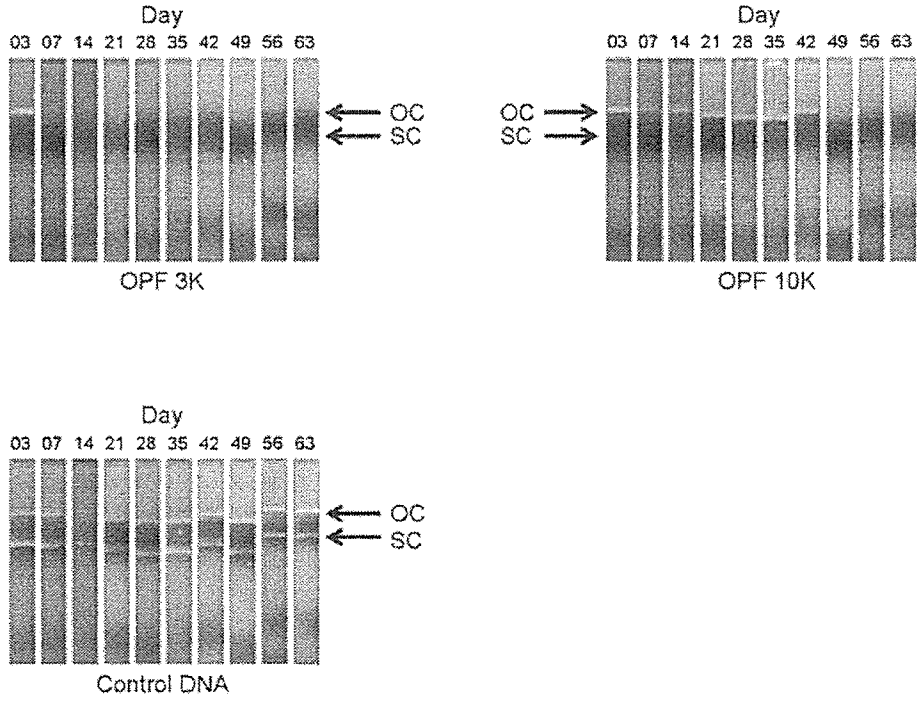

Figure 3. Agarose gels following electrophoresis of plasmid DNA released from OPF hydrogels in enzymatic PBS (pH 7.4) *in vitro* and control DNA (unencapsulated, nonreleased). The arrows indicate the migration distances for open-circular DNA (OC) and super-coiled DNA (SC).

49–84 for initial DNA loadings of 10 and 100 μg DNA, respectively ($p < 0.05$). There was no significant difference, however, in the cumulative fraction of DNA released, as determined by OliGreen or PicoGreen, at any time point in the case of composites in which DNA (10 μg) was loaded into the CGMS component ($p < 0.05$).

All of the OPF 10K release samples completely degraded by day 63. Additionally, all of the release samples from composite groups completely degraded by day 84. The OPF 3K release samples, however, persisted until day 147.

The release of DNA from OPF 10K samples and from composites in which the DNA was loaded into the OPF component presented similar profiles (Fig. 2). The release profiles of the OPF 3K and of the composites in which the DNA was loaded into the CGMS component were each unique from the release profiles of the other groups. A small initial burst release was observed from all groups at day 3, with the release from the composites in which 10 μg DNA was loaded into the CGMS component being significantly lower than the release from all other groups at this time point ($p < 0.05$). The cumulative release of DNA from composites in which 10 μg DNA was loaded into the CGMS component was significantly lower than the release from OPF 10K as well as the composites in which DNA was loaded into the OPF component at all relevant time points, as determined by PicoGreen, and at all time points except day 21 for OPF 10K and days 14 and 21 for composites (100 μg DNA in OPF), as determined by OliGreen ($p < 0.05$). The cumulative release of DNA from OPF 3K samples was significantly less than that from OPF 10K (day 14 and onward) and from composites in which 10 μg DNA (day 7 and onward) and 100 μg DNA (day 14 and onward) was loaded into the OPF component, as determined by both assays ($p < 0.05$).

Gel electrophoresis of released DNA

The structural integrity of plasmid DNA released *in vitro* from OPF 3K and OPF 10K (Fig. 3) and from composites of OPF and CGMS (Fig. 4) was assessed through agarose gel electrophoresis. The lanes on each gel corresponding to the material control groups into which no plasmid DNA was loaded did not exhibit any fluorescent bands (data not shown). The control plasmid DNA (nonentrapped, nonreleased) was present in both super-coiled and open-circular conformations at all time points (Figs. 3 and 4). Plasmid DNA released from composites of OPF and CGMS in which 100 μg DNA had been loaded into the OPF was predominately in the open-circular conformation over the course of the study, with a band of super-coiled DNA present for days 3 through 42. A band of linear

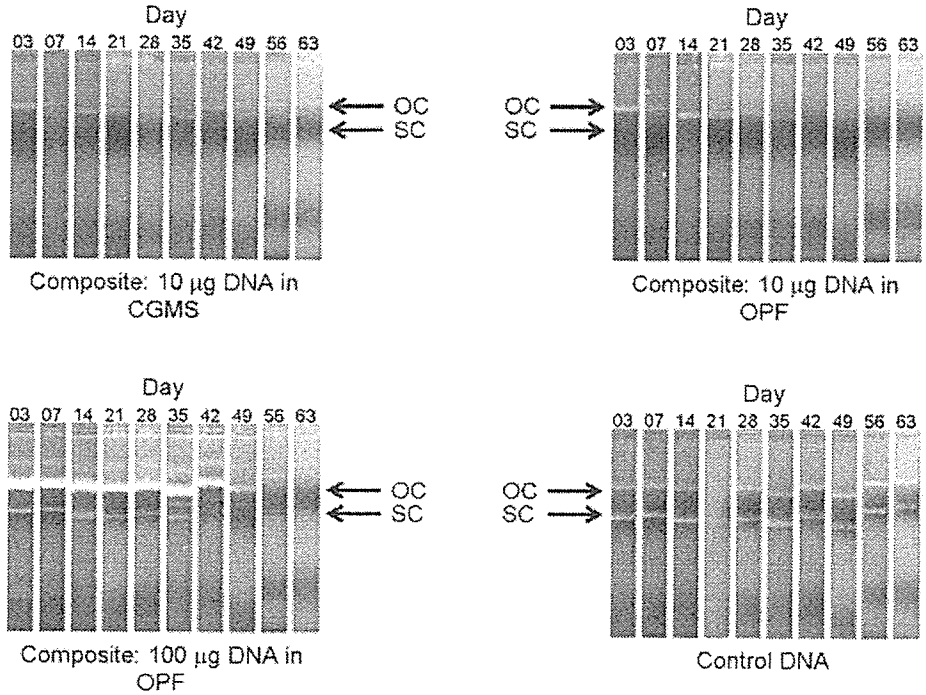

Figure 4. Agarose gels following electrophoresis of plasmid DNA released from hydrogel composites of OPF and CGMS in enzymatic PBS (pH 7.4) *in vitro* and control DNA (unencapsulated, nonreleased). The arrows indicate the migration distances for open-circular DNA (OC) and super-coiled DNA (SC).

DNA was observed for this group at days 28 through 42. Plasmid DNA released from composites of OPF and CGMS in which 10 μg DNA had been loaded into the CGMS was present predominately in the open-circular conformation over the course of the study from days 3 through 35, after which no bands were visually apparent for this group. In the case of composites of OPF and CGMS in which 10 μg DNA was loaded into the CGMS, the released DNA was consistently present in an open-circular conformation for the duration of the study (days 3–63). DNA released from OPF 10K alone was predominant in the open-circular conformation over the course of the study, with a faint super-coiled band at days 3 through 21 and a faint linear band at days 35 and 42. The DNA released from OPF 3K alone was predominately in the open-circular conformation with visible bands at days 3, 7, 28, 56, and 63.

Hydrogel swelling

The swelling ratio of each release sample was calculated over the course of the release study. All swelling ratio profiles exhibited a slight increase from an initial positive value to a maximum value, followed by a steady decrease in swelling ratio with time to approach a value of −1.0 upon complete degradation (Fig. 5). In general, no significant differences were present between the swelling ratio of samples containing DNA and their respective blanks ($p < 0.05$). The composite groups containing DNA exhibited the same general swelling ratio profiles, with no significant difference between them at any time point, with the exception of day 14 ($p < 0.05$). Although the swelling ratio profiles of the OPF 10K groups approached a value of −1.0 more rapidly than did the composite groups, few significant differences existed between the OPF 10K groups and the composite groups before day 49 ($p < 0.05$). However, the swelling ratio of the OPF 10K samples with DNA was significantly lower than that of the composites with 10 μg DNA in CGMS and 10 μg DNA in OPF at days 49–63 and the composites with 100 μg DNA in OPF at day 49 ($p < 0.05$).

The initial swelling ratios (day 3) of all OPF 10K and composite groups were significantly greater than the swelling ratios of each OPF 3K group ($p < 0.05$), with the initial swelling ratio of the OPF 3K samples being approximately half of the value for other groups. The swelling ratio of the OPF 10K and composite groups then increased to a maximum value at day 7 (day 14 for composites with 100 μg DNA loading in OPF), followed by sustained decreases in swelling ratio values until approaching a value of −1.0 upon degradation. The swelling ratio of OPF 3K samples, however, increased slowly with time to maximum values at day 77, followed by sustained decreases in swelling ratio

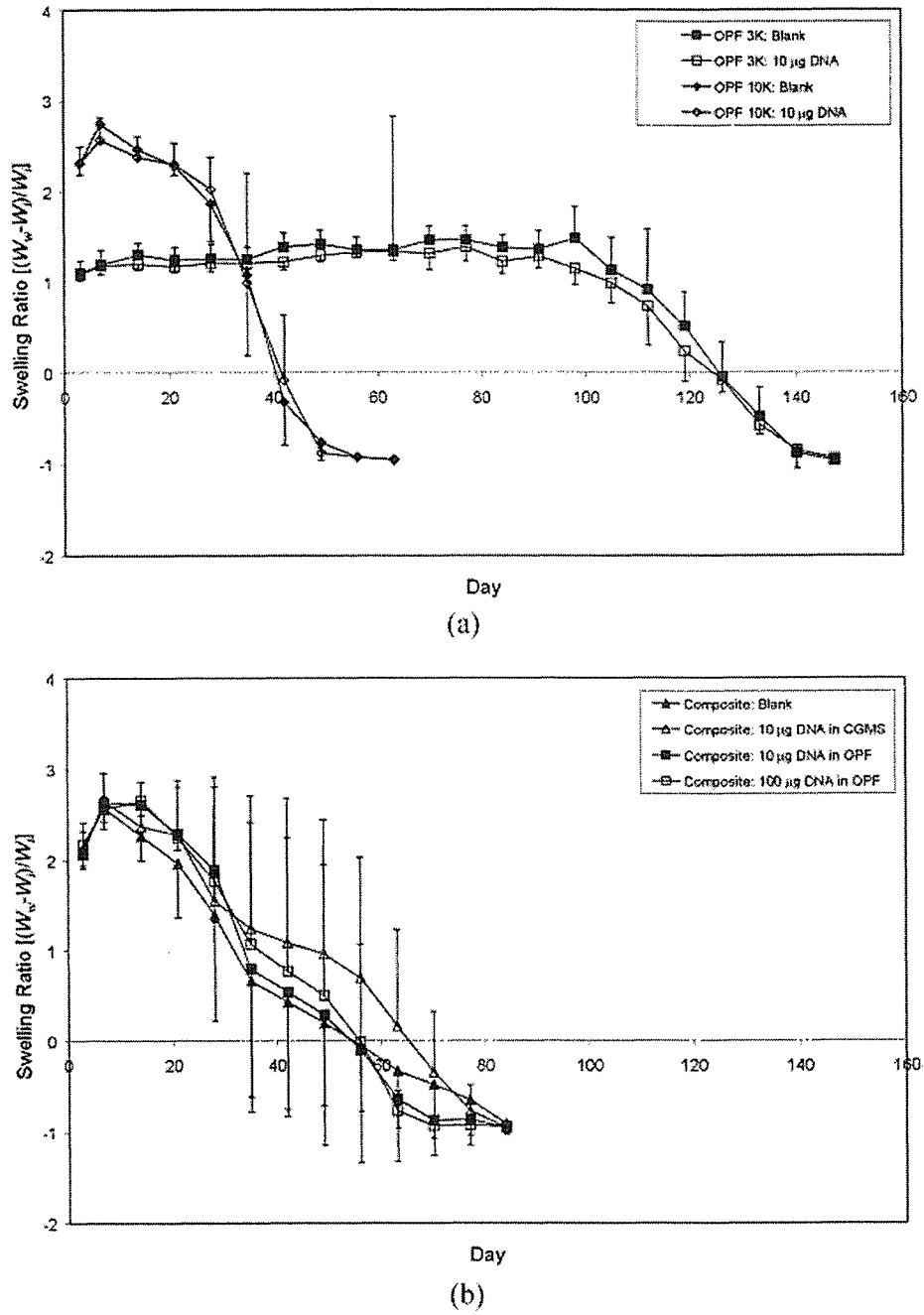

Figure 5. Swelling ratio profiles of OPF hydrogels (a) and of hydrogel composites of OPF and CGMS (b) in enzymatic PBS (pH 7.4) (n = 6). The DNA release profiles were measured from these samples. Error bars represent ± standard deviation.

values to approach a value of −1.0 upon complete degradation at day 147.

By the time the OPF 10K samples completely degraded at day 63, the swelling ratio of the blank samples and samples containing DNA reached values of approximately −1. The composite group samples required a longer amount of time for degradation, being completely degraded at day 84, at which the swelling ratios were approximately −1. The OPF 3K samples required the longest time to degrade, with complete degradation of all samples noted at day 147, with final swelling ratios of approximately −1.

Hydrogel polymer mass loss

The polymer mass loss of three samples from each group at each time point was examined (Fig. 6). The

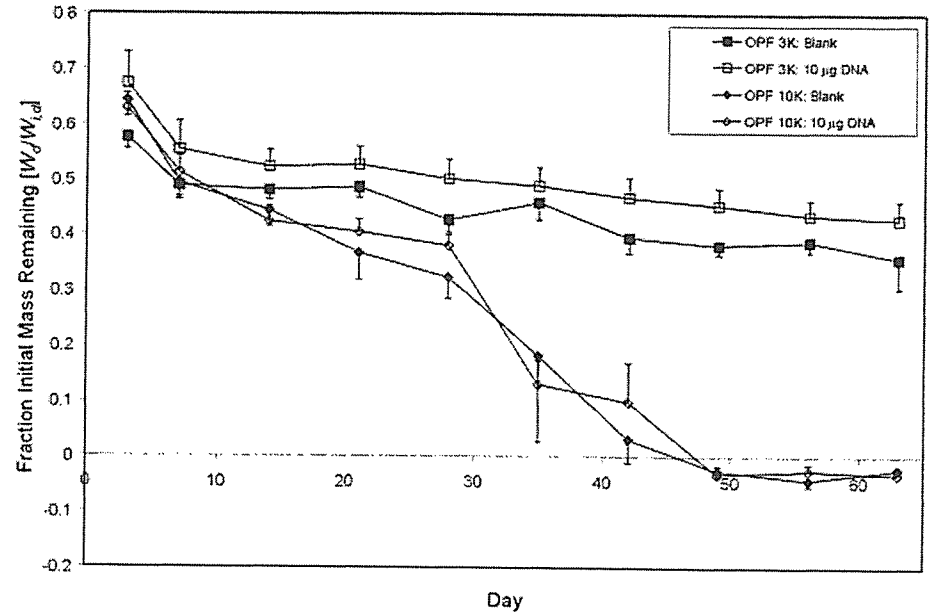

Figure 6. Profile of the fraction of initial polymer mass remaining for OPF hydrogels (a) and composites of OPF and CGMS (b) in enzymatic PBS (pH 7.4) (n = 3/time point). Error bars represent ± standard deviation.

average initial dry polymer mass for each group was determined from six samples that were lyophilized immediately after fabrication. The most marked degree of mass loss in any one period occurred in the first three days. The mass loss from OPF 10K samples and from composite groups continued in a steady fashion from day 3 through day 63 (Fig. 6). All of the OPF 10K samples and some of the samples from each of the composite groups were completely degraded by day 63, whereas none of the OPF 3K samples were completely degraded at this time point. In general, the mass loss within a group was not significantly different at any given time point between a DNA loaded sample and the corresponding blank sample for OPF 10K and composite groups ($p < 0.05$). This was not the case for the OPF 3K group, in which the DNA loaded samples retained significantly more mass than the blank OPF 3K samples at each time point, except days

7, 35, and 63 ($p < 0.05$). The fraction of the initial mass remaining of OPF 3K samples loaded with DNA was significantly greater than that of OPF 10K samples loaded with DNA from day 14 onward, with the exception of day 35 ($p < 0.05$). Additionally, the fraction of the initial mass remaining of OPF 3K samples loaded with DNA was significantly higher than that of composites with 10 μg DNA loaded into the CGMS at days 14 and 42–56 and composites with 10 μg DNA or 100 μg DNA loaded into the OPF at days 14–63 and days 14 and 42–63, respectively ($p < 0.05$).

DISCUSSION

Hydrogels of OPF have been shown to release bioactive DNA in a controlled fashion[17]; yet the lack of pore volume into which tissue might infiltrate limits the potential of OPF hydrogels alone to serve as viable tissue engineering scaffolds. In a subsequent effort to create porous OPF scaffolds, composites of OPF and CGMS were fabricated and examined for controlled DNA release *in vivo*.[18] Specifically, the release of radiolabeled plasmid DNA from CGMS groups (3 and 6 m*M*), groups of composites of OPF 10K and CGMS (3 and 6 m*M*), and from OPF 10K was characterized in a subcutaneous murine model. Additionally, the degradation of radiolabeled CGMS from the same groups was examined.[18] It was shown that the composites of OPF 10K and CGMS extend the bioavailability of DNA relative to CGMS alone and injection of DNA solution.[18] Further, the encapsulation of CGMS in OPF was shown to extend the apparent persistence of the cationized gelatin, relative to injection of CGMS alone.[18] No significant difference was noted in the DNA release between the composite groups (DNA loaded into CGMS) and the OPF 10K alone.[18] It was proposed that control of the release of DNA from the composites was dominated by the degradation of the OPF network, but the characterization of the degradation of OPF *in vivo* was not undertaken in that study.[18] As a result, the present study sought to expand upon the previous work through characterization of the release of DNA from composites of OPF 10K and CGMS (6 m*M*) and characterization of the swelling and degradation properties of these composites. Thus, comparison of the observed DNA release from the composites with the degradation of the composite could be achieved, as could comparison with the release, swelling, and degradation properties of material control groups (OPF 3K and OPF 10K).

In the present study, the release of DNA from composites of OPF 10K and CGMS, in which DNA was loaded into the OPF component, and from control OPF 10K samples followed similar profiles, with the OPF 10K samples reaching a final cumulative release value slightly before the composite formulations. Although enzymes such as collagenase can readily enter the OPF network to facilitate degradation of the gelatin microspheres, the mesh size of OPF 10K hydrogels (13.6 ± 0.3 nm[23]) is much smaller than the apparent molecular size of plasmid DNA (on the order of hundreds of nanometers[4,24]) and the apparent molecular size of plasmid DNA-cationized gelatin complexes.[4] It follows that the degradation of the OPF network likely dominates the release of plasmid DNA, as size limitations presented by the small mesh size of OPF relative to the larger size of plasmid DNA and plasmid DNA-cationized gelatin microsphere complexes likely serve as a significant barrier to the release of plasmid DNA by simple diffusion.[18]

Despite the similarities between the release of DNA from composites in which DNA was loaded into the OPF and the release from the control OPF 10K, significant differences were observed between the release of plasmid DNA from composites in which the DNA was loaded into the CGMS and from the control OPF 10K. The formation of complexes between plasmid DNA and CGMS upon loading contributed to the smaller burst release of DNA at day 3, and a slower DNA release rate was observed from composites in which plasmid DNA was loaded into the CGMS (relative to OPF 10K and composites in which DNA was loaded into the OPF component) (Fig. 2). Loading of CGMS with DNA occurred through reconstitution of freeze-dried CGMS in a volume of DNA solution less than the equilibrium swelling volume for the given mass of CGMS. As a result, the solution was completely incorporated into the CGMS. It follows that the DNA was fully associated with the CGMS after loading, be it within the microspheres or on the surface of the microspheres.[18] Release of the DNA associated with the CGMS in the composite would require either dissociation of the DNA from the cationized gelatin and/or degradation of the cationized gelatin. In either case, the DNA or DNA-cationized gelatin complexes would likely be entrapped within the OPF matrix, due to previously discussed size considerations, until degradation of the network. Thus, the small burst release at day 3 of DNA from the composites in which DNA was loaded into the CGMS component likely stemmed from dissociation of DNA from CGMS at or near the surface of the composite.

The requirement for DNA to be liberated from the CGMS prior to release from the OPF network in the composite group in which DNA was loaded into the CGMS component contributes to the observed slower release rate relative to the other composite groups and the control OPF 10K. Interestingly, the total cumulative release observed from the composite group in which DNA was loaded into the CGMS component was only $71.9 \pm 5.0\%$ upon complete degradation of these samples. Potential differences between the ac-

tual DNA loading per composite and the volumetrically calculated loading values will contribute to this observation. Such differences would be expected to be most pronounced in this group, in which the DNA was loaded solely within the CGMS component of the composite. Any inhomogeneity either in the loading of DNA within the CGMS or in the distribution of the CGMS within the uncrosslinked solution prior to fabrication of the samples would affect the validity of the volumetric calculations of DNA loading. However, the use of volumetric calculations to estimate DNA loading in OPF networks without a CGMS component has been validated previously.[17] It is expected that loading of DNA within the OPF component of composites would present less margin for error in determination of DNA loading through volumetric calculation than would loading of the DNA into the CGMS component, as OPF forms the bulk of the composite, and the DNA solution should distribute homogeneously throughout the OPF solution prior to crosslinking. Interestingly, the final cumulative release of DNA from hydrogels of OPF without a CGMS component exceeded the volumetrically calculated initial DNA loading of these samples. Although an under-calculation in determination of the initial DNA loading could contribute to this observation, the exact reason for the final cumulative release surpassing the calculated initial loading for these samples was not determined. However, the release profiles and final cumulative release values obtained for these samples were highly reproducible, as evident from the small error for these groups (Fig. 2).

The release of DNA from OPF 3K hydrogels, following an initial burst at day 3, occurred in a sustained, linear fashion through day 70 (Fig. 2). From day 70 onward, the release of DNA from OPF 3K proceeded at an increased rate until complete degradation of the gels was noted at day 147. The profile of DNA release from OPF 3K hydrogels was markedly different from the DNA release profiles from OPF 10K gels and composites of OPF 10K and CGMS (Fig. 2). The data suggest that a significantly lower extent of swelling coupled with slower degradation kinetics contributed to the observed slower release of DNA from OPF 3K gels than from OPF 10K gels and composites. The swelling ratio of each release sample was tracked over the course of the study (Fig. 5). This value reflects the change in the mass of a gel at each time point, with respect to the initial mass of the gel. Positive swelling ratio values reflect an increase in the mass of a gel due to an increase in the volume of incorporated solution as the gel swells. Conversely, negative swelling ratio values reflect either a decrease in the polymer content of the gel, a decrease in the solution content of the gel, or a decrease in both the polymer and solution content of a gel. As a hydrogel degrades, the wet weight of the gel approaches zero. Thus, the value of the swelling ratio approaches a value of -1 upon hydrogel degradation. Indeed, the swelling ratio of all gels in the present study reached final values of approximately -1 (Fig. 5).

Comparison of the swelling ratio of the gels within a group (Fig. 5) with the corresponding profile of DNA release (Fig. 2) demonstrates a strong relationship between the release of DNA and the swelling ratio of the gels. The OPF 10K gels were the first to completely degrade, to reach a swelling ratio value of approximately -1, and to reach their final cumulative DNA release value, followed by the composites in which DNA was loaded in the OPF component and CGMS component, respectively (Figs. 2 and 5). The OPF 3K gels, however, exhibited a slight, steady increase in swelling ratio values from day 3 through approximately day 77, followed by a distinctly faster decrease in swelling ratio values to approach a value of -1 at day 147 (Fig. 5). A corresponding slow, sustained release of DNA from OPF 3K gels was observed from day 3 through approximately day 72, followed by a marked increase in the rate of DNA release thereafter (Fig. 2). However, the degradation of OPF 3K hydrogels and the release of DNA from OPF 3K gels occurred at a much slower rate than previously observed *in vitro*.[17] Differences with previous reports in the degradation and DNA release kinetics of OPF 3K hydrogels could be influenced by the presence of collagenase in the release buffer in the present study and variability in batches of polymer synthesis, among other factors. However, in all cases, the release of DNA from OPF hydrogels was directly related to the degradation of the hydrogels as marked by visual examination and swelling ratio values, indicating that control of the release of plasmid DNA from OPF hydrogels is dominated by the degradation of the gels.[17]

Although the swelling ratio reflects the degradation of a gel with time, it does not allow for differentiation between changes due to loss of polymer mass and loss of solution mass as the swelling ratio value decreases. As a result, a set of samples were fabricated to allow for the determination of polymer mass loss with time for the various groups. Based upon the results of previous studies examining the release kinetics of DNA from composites of OPF and CGMS *in vivo* and from OPF 3K and OPF 10K *in vitro*, it was expected that all samples from each group would completely degrade by day 63.[17,18] As a result, a number of samples sufficient for characterization of the polymer mass loss through day 63 were fabricated at the onset of the study. As seen in Figure 6, all samples lost ~30–40% of the initial polymer mass by day 3. This loss of mass can be attributed to extraction of the sol fraction, composed of polymer chains that did not crosslink to incorporate into the hydrogel network.[25] The OPF 10K samples and the composite samples, in general, had approximately zero percent of the initial